Mesoscopic Sensitivity of Speckles in Disordered Nonlinear Media to Changes of the Scattering Potential

B. Spivak
Physics Department, University of Washington, Seattle, Washington 98195

A. Zyuzin
A. F. Ioffe Institute, 194021 St. Petersburg, Russia
(Received 30 April 1999)

We show that the sensitivity of wave speckle patterns in disordered nonlinear media to changes of scattering potential increases with sample size. For large sizes the sensitivity diverges, which implies that for a given coherent wave incident on a sample there are multiple solutions for the spatial distribution of the wave density. The number of solutions increases exponentially with the sample size.

PACS numbers: 72.10.Fk, 72.20.Ht

If a coherent wave described by a field $\phi(\boldsymbol{r})$ propagates in an elastically scattering medium, the spatial dependence of its "density" $n(\boldsymbol{r}) = |\phi(\boldsymbol{r})|^2$ exhibits speckle: $n(\boldsymbol{r})$ is a random, sample specific function of coordinate $\boldsymbol{r}$. In the cases of noninteracting electrons and electromagnetic waves propagating in linear media the theory of sensitivity of speckle patterns to a change in scattering potential was developed long ago [1–5]. It was shown that the sensitivity is very large, but finite.

In this Letter we consider the same question in the case where a wave propagates in nonlinear media. For the sake of concreteness we consider the situation where the propagation of the wave is described by a nonlinear Schrödinger equation

$$\left(-\frac{1}{2m}\frac{\partial^2}{\partial \boldsymbol{r}^2} - \epsilon + u(\boldsymbol{r}) + \beta n(\boldsymbol{r})\right)\phi(\boldsymbol{r}) = 0. \qquad (1)$$

Here m is the wave mass, ϵ is the wave's energy, β is a constant, and $u(\boldsymbol{r})$ is a scattering potential which is a random function of the coordinates. Similar equations appear in the theory of electromagnetic waves propagating in nonlinear media [6], the theory of hydrodynamic turbulence [7], and the theory of turbulent plasma [8]. We will assume white noise statistics in $u(\boldsymbol{r})$: $\langle u(\boldsymbol{r})\rangle = 0$, $\langle u(\boldsymbol{r})u(\boldsymbol{r}_1)\rangle = (\pi/lm^2)\delta(\boldsymbol{r} - \boldsymbol{r}_1)$. Here angular brackets correspond to averaging over realizations of $u(\boldsymbol{r})$ and l is the elastic mean free path [$l \gg k^{-1} = (2\epsilon m)^{-1/2}$].

Let us consider the case where a coherent wave $\phi_0(\boldsymbol{r}) = \sqrt{n_0}\exp(i\boldsymbol{k}\cdot\boldsymbol{r})$ with momentum $\boldsymbol{k}$ is incident on a disordered sample of the dimension $L \gg l$ (see the inset in Fig. 1). We will show that the sensitivity of the nonlinear speckle pattern $n(\boldsymbol{r})$ to a small change in $u(\boldsymbol{r})$ increases with sample size L. At arbitrarily small n_0 and for an arbitrary sign of β the sensitivity becomes infinite provided L is large enough. This implies that Eq. (1) has many solutions at a given coherent wave incident on a sample. This is very different from the case of uniform nonlinear media, where types of instabilities depend on the sign of β. (See, for example, [6].)

The $\boldsymbol{r}$ dependence of the average density $\langle n(\boldsymbol{r})\rangle$ can be described by the diffusion equation, which is equivalent to calculation of the diagrams shown in Fig. 2(a). We use the usual diagram technique for averaging over realizations of random potential [9]. If $|\beta n_0| \ll \sqrt{\epsilon k/lm}$ one can neglect the nonlinear corrections to the diffusion coefficient $D = lk/3m$. We obtained this criterion by calculating the transport scattering cross section on the effective potential $\beta n(\boldsymbol{r})$. To do so we used calculated in [4,10] spatial correlation functions of the density fluctuations on scale smaller than mean free path [11]. In the case of the sample geometry shown in the inset of Fig. 1, we have $\langle n(\boldsymbol{r})\rangle = n_0$.

We can characterize the speckle pattern $n(\boldsymbol{r})$ by correlation functions $\langle \delta n(\boldsymbol{r})\delta n(\boldsymbol{r}_1)\rangle$, where $\delta n(\boldsymbol{r}) = n(\boldsymbol{r}) - \langle n(\boldsymbol{r})\rangle$. To calculate it at $|\boldsymbol{r} - \boldsymbol{r}_1| \gg l$ one can use the Langevin approach [4,11]

$$\frac{d}{d\boldsymbol{r}}\,\delta\boldsymbol{J}(\boldsymbol{r}) = 0; \qquad \delta\boldsymbol{J}(\boldsymbol{r}) = -D\frac{d}{d\boldsymbol{r}}\,\delta n(\boldsymbol{r}) + \boldsymbol{J}_{\mathrm{ext}}(\boldsymbol{r},\{u\}); \qquad (2)$$

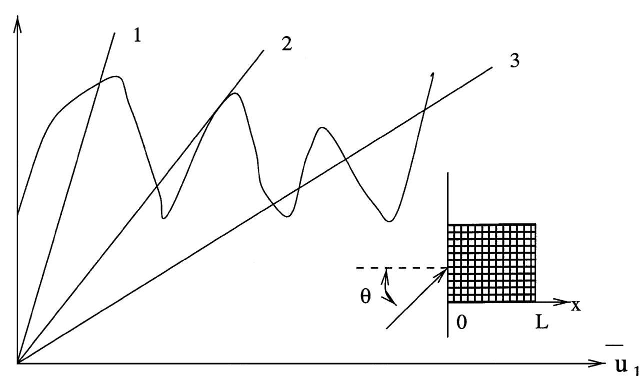

FIG. 1. Graphical solution of Eq. (16). The wavy line corresponds to $F_1(\overline{u}_1)$, while straight lines 1 and 3 correspond to $\gamma^{-1/2}\overline{u}_1$ in the cases $\gamma \sim 1$ and $\gamma \gg 1$, respectively. Line 2 illustrates the case where a solution of Eq. (16) is unstable. The inset shows the sample geometry.

 0031-9007/00/84(9)/1970(4)$15.00

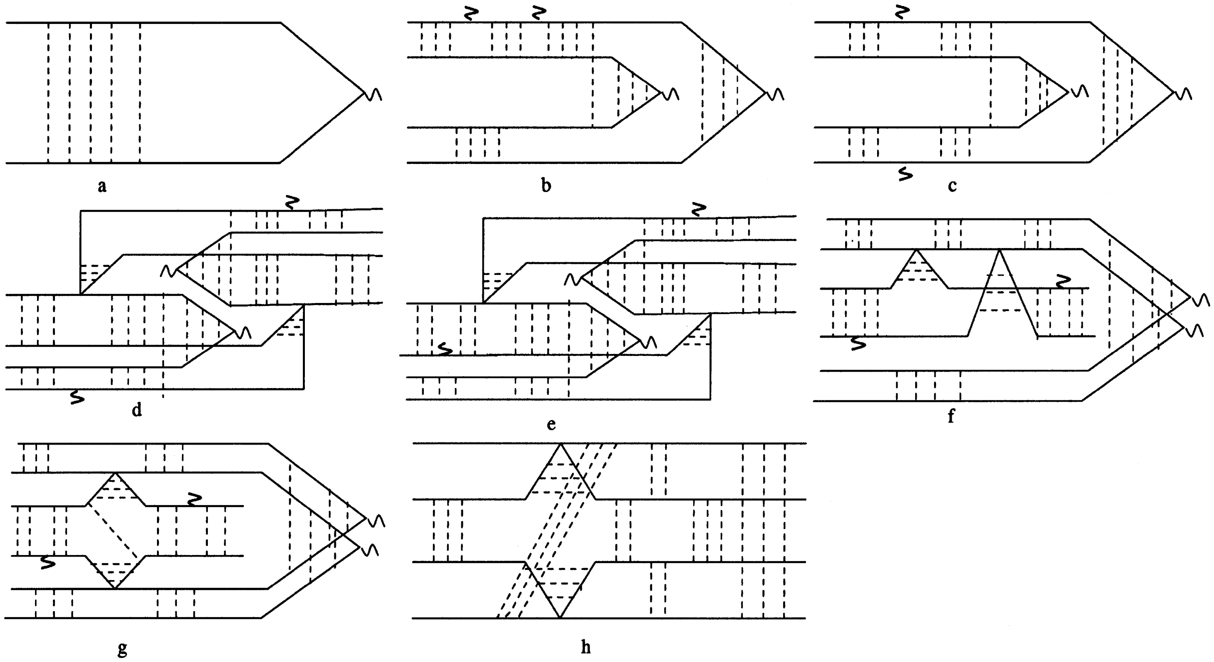

FIG. 2. Solid lines correspond to Green functions of Eq. (1) with $\beta = 0$, dashed lines correspond to $(\pi/lm^2)\delta(\boldsymbol{r} - \boldsymbol{r}_1)$, the four solid lines' vertices correspond to the factor β, thick wavy lines correspond to $\Delta u(\boldsymbol{r})$, and thin wavy lines correspond to density vertices.

$$\langle J^i_{\text{ext}}(\boldsymbol{r},\{u\})J^j_{\text{ext}}(\boldsymbol{r}_1,\{u\})\rangle = \frac{2\pi l}{3m^2}\langle n(\boldsymbol{r})\rangle^2 \delta(\boldsymbol{r} - \boldsymbol{r}_1)\delta_{ij}\,. \tag{3}$$

Here $\boldsymbol{J}(\boldsymbol{r}) = \frac{1}{2m}\,\text{Im}\phi^*(\boldsymbol{r})\,(d/d\boldsymbol{r})\phi(\boldsymbol{r})$ is the current density, $\delta\boldsymbol{J}(\boldsymbol{r}) = \boldsymbol{J}(\boldsymbol{r}) - \langle \boldsymbol{J}(\boldsymbol{r})\rangle$, $\boldsymbol{J}_{\text{ext}}(\boldsymbol{r},\{u\})$ is a random external current source, and $\langle \boldsymbol{J}_{\text{ext}}(\boldsymbol{r},\{u\})\rangle = 0$. As a result we have

$$\langle \delta n(\boldsymbol{r})\delta n(\boldsymbol{r}_1)\rangle = \frac{6\pi n_0^2}{k^2 l}\,G(\boldsymbol{r},\boldsymbol{r}') \sim \frac{n_0^2}{k^2 l|\boldsymbol{r} - \boldsymbol{r}_1|}\,, \tag{4}$$

where $G(\boldsymbol{r},\boldsymbol{r}_1)$ is the Green function of the equation

$$-\frac{d^2}{d^2\boldsymbol{r}}\,G(\boldsymbol{r},\boldsymbol{r}_1) = \delta(\boldsymbol{r} - \boldsymbol{r}_1) \tag{5}$$

with boundary conditions: $G(\boldsymbol{r},\boldsymbol{r}') = 0$ at open boundary and $\boldsymbol{n}\cdot\frac{\partial}{\partial \boldsymbol{r}}G(\boldsymbol{r},\boldsymbol{r}') = \boldsymbol{n}\cdot\frac{d}{\partial \boldsymbol{r}}\langle n(\boldsymbol{r})\rangle = 0$ at the closed sample's boundaries.

A change of scattering potential $\Delta u(\boldsymbol{r}) = u'(\boldsymbol{r}) - u(\boldsymbol{r})$ leads to a change of speckle pattern $\Delta n(\boldsymbol{r}) = n(\boldsymbol{r},\{u'\}) - n(\boldsymbol{r},\{u\})$. Here $n(\boldsymbol{r},\{u'\})$ and $n(\boldsymbol{r},\{u\})$ are solutions of Eq. (1) with scattering potentials $u'(\boldsymbol{r})$ and $u(\boldsymbol{r})$, respectively.

We can characterize the sensitivity of speckle pattern to change in scattering potential by a correlation function $K(\boldsymbol{r},\boldsymbol{r}_1) = \langle\langle \Delta n(\boldsymbol{r})\Delta n(\boldsymbol{r}_1)\rangle\rangle$. Here double angular brackets correspond to averaging over both realizations of $u(\boldsymbol{r})$ and realizations of $\Delta u(\boldsymbol{r})$. We assume that $\langle\langle \Delta u(\boldsymbol{r})\Delta u(\boldsymbol{r}_1)\rangle\rangle = U^2\exp(-|\boldsymbol{r} - \boldsymbol{r}_1|/r_0)$, $r_0 \gg l$.

To obtain the value of $K(\boldsymbol{r},\boldsymbol{r}_1)$ at $|\boldsymbol{r} - \boldsymbol{r}_1| \gg l$ and in quadratic in $\Delta u(\boldsymbol{r})$ approximation one can generalize the Langevin approach

$$\begin{aligned}\boldsymbol{J}_{\text{ext}}(\boldsymbol{r},\{u'\}) &= \boldsymbol{J}_{\text{ext}}(\boldsymbol{r},\{u\}) \\ &\quad + \int d\boldsymbol{r}'\,\frac{\delta \boldsymbol{J}_{\text{ext}}(\boldsymbol{r},\{u\})}{\delta u(\boldsymbol{r}')} \\ &\quad \times [\Delta u(\boldsymbol{r}') + \beta\Delta n(\boldsymbol{r}')]\,,\end{aligned} \tag{6}$$

$$\begin{aligned}\left\langle \frac{\delta J^i_{\text{ext}}(\boldsymbol{r},\{u\})}{\delta u(\boldsymbol{r}')}\,\frac{\delta J^j_{\text{ext}}(\boldsymbol{r}_1,\{u\})}{\delta u(\boldsymbol{r}_1')}\right\rangle &= \frac{6\pi}{lk^2}\,\delta_{ij}\delta(\boldsymbol{r} - \boldsymbol{r}_1)\{G(\boldsymbol{r}',\boldsymbol{r}_1')\langle n(\boldsymbol{r})\rangle[\langle n(\boldsymbol{r}_1')\rangle G(\boldsymbol{r}',\boldsymbol{r}) + \langle n(\boldsymbol{r}')\rangle G(\boldsymbol{r}_1',\boldsymbol{r})] \\ &\quad - [\langle n(\boldsymbol{r}')\rangle\langle n(\boldsymbol{r}_1')\rangle G(\boldsymbol{r}',\boldsymbol{r})]G(\boldsymbol{r}_1',\boldsymbol{r})\}\,, \\ \left\langle \frac{\delta \boldsymbol{J}_{\text{ext}}(\boldsymbol{r},\{u\})}{\delta u(\boldsymbol{r}')}\right\rangle = \left\langle J^i_{\text{ext}}(\boldsymbol{r},\{u\})\,\frac{\delta J^j_{\text{ext}}(\boldsymbol{r}',\{u\})}{\delta u(\boldsymbol{r}_1)}\right\rangle &= 0\,.\end{aligned} \tag{7}$$

Equations (2)–(7) are a closed system which differs from that in [4,10] by the term in Eq. (6) proportional to β. The equations are equivalent to the summation of diagrams shown in Figs. 2(b)–2(g). Diagrams, shown in Fig. 2(h), are responsible for the small non-Gaussian part of the distribution function of $\delta\boldsymbol{J}_{\text{ext}}(\boldsymbol{r},\{u\})/\delta u(\boldsymbol{r}')$. They are proportional to a small parameter $1/k^2 lL \ll 1$ in the three dimensional case ($d = 3$) and can be neglected. All diagrams responsible for localization effects can be neglected as well. One can expand $K(\boldsymbol{r},\boldsymbol{r}_1) = \sum_{k=0}^{\infty} K^{(k)}(\boldsymbol{r},\boldsymbol{r}_1)$ in powers of β^2, where $K^{(k)}$ is a part of the correlation function proportional to β^{2k}.

Let us first consider the linear case $\beta = 0$. Index (0) will indicate quantities calculated at $\beta = 0$. Solving Eqs. (2), (3), (6), and (7) in $d = 3$ case we get [4]

$$K^{(0)}(\boldsymbol{r},\boldsymbol{r}_1) = \langle\langle \Delta n^{(0)}(\boldsymbol{r}) \Delta n^{(0)}(\boldsymbol{r}_1)\rangle\rangle \sim \left(\frac{\tau_D}{\tau_f}\right)^2 \langle \delta n(\boldsymbol{r}) \delta n(\boldsymbol{r}_1)\rangle. \tag{8}$$

Here the ratio between $\tau_D = L^2/D$ and $\tau_f = L/r_0 U$ characterizes the sensitivity of speckle to variation in scattering potential. The case, when the ratio is $\tau_D/\tau_f \sim 1$, corresponds to a complete change in the speckle pattern due to the change of the scattering potential $\Delta u(\boldsymbol{r})$. We therefore define the sensitivity as $(\tau f/\tau_D)^2 K(\boldsymbol{r},\boldsymbol{r}')$. Equation (8) can also be obtained by calculating the diagrams shown in Figs. 2(b) and 2(c). One can get the same estimate from the requirement that an additional phase $|\chi^{(0)}| \sim \sqrt{\tau_D/\tau_f}$, which the traveling wave acquires due to the change in the potential $\Delta u(\boldsymbol{r})$, is of order π.

Let us now turn to the case $\beta \neq 0$. Expanding Eqs. (2)–(6) in β, and performing the average over realizations of $u(\boldsymbol{r})$ and $\Delta u(\boldsymbol{r})$ in the $d = 3$ case we get, for example,

$$K^{(1)}(\boldsymbol{r},\boldsymbol{r}_1) \sim \gamma K^{(0)}(\boldsymbol{r},\boldsymbol{r}_1), \tag{9}$$

where

$$\gamma = \left(\frac{3}{2}\frac{n_0 \beta}{\epsilon}\right)^2 \left(\frac{L}{l}\right)^3. \tag{10}$$

Equation (9) can also be obtained by calculating the diagrams shown in Figs. 2(d)–2(g) or by estimating the additional phase which the wave traveling along a typical diffusion path will pick up due to the change in the effective potential $\beta \Delta n^{(0)}(\boldsymbol{r})$

$$\langle\langle (\Delta\chi^{(1)})^2\rangle\rangle = \left(\frac{k\beta}{2\epsilon}\right)^2 \left\langle\left\langle \int ds\, ds_1\, \Delta n^{(0)}(\boldsymbol{r}(s)) \times \Delta n^{(0)}(\boldsymbol{r}(s_1))\right\rangle\right\rangle \sim \gamma \langle\langle (\chi^{(0)})^2\rangle\rangle. \tag{11}$$

Here integration is taken along a typical diffusion path.

Equations (9) and (11) imply that at $\gamma \gg 1$ the perturbation theory with respect to γ diverges. Consequently, the sensitivity $(\tau_f/\tau_D)^2 K(\boldsymbol{r},\boldsymbol{r}')$ diverges at $\gamma \sim 1$. We will show that this is a consequence of the fact that at $\gamma > 1$ Eq. (1) has many solutions. To describe these solutions we have to use nonperturbative analysis.

It is convenient to expand

$$\beta n(\boldsymbol{r}) = \frac{D}{\sqrt{L}} \sum_{m=1}^{\infty} m^{1/3} \overline{u}_m n_m(\boldsymbol{r}) \tag{12}$$

over a complete set of eigenstates $n_m(\boldsymbol{r})$ of diffusion equation

$$-D \frac{d^2}{d^2\boldsymbol{r}} n_m(\boldsymbol{r}) = E_m n_m(\boldsymbol{r}), \tag{13}$$

where $E_m \sim \tau_D^{-1} m^{2/3}$ are eigenvalues of Eq. (13) and $m = 1, 2, \ldots$ labels the eigenstates.

Let us first substitute Eq. (12) into Eq. (1) and regard $\overline{u}_m$ as independent parameters. Then Eq. (1) becomes a linear equation. Denoting the solution of Eq. (1) as $\phi(\boldsymbol{r},\{\beta n\})$ we can write the self-consistency equation $n(\boldsymbol{r}) = |\phi(\boldsymbol{r},\{\beta n\})|^2$ as

$$\gamma^{-1/2} m^{2/3} \overline{u}_m = F_m(\overline{u}_1, \ldots, \overline{u}_k, \ldots), \tag{14}$$

which is equivalent to Eq. (1). Here $F_m(\overline{u}_1,\ldots) = kL^{-1} n_0^{-1} m^{1/3} l^{1/2} \int d\boldsymbol{r}\, |\phi(\boldsymbol{r},\{\beta n\})|^2 n_m(\boldsymbol{r})$ are random sample specific functions, whose forms depend on realizations of $u(\boldsymbol{r})$.

The problem of the investigation of properties of $F_m(\overline{u}_1,\ldots)$ as a function of $\overline{u}_n$ is equivalent to the linear problem considered in [1–5]. To characterize the dimensionless functions F_m we calculate the following correlation functions with the help of Eqs. (2)–(5) and (7): (a) mesoscopic fluctuations of modes with $m \neq n$ are uncorrelated $\langle \delta F_m \delta F_n\rangle = 0$, where $\delta F_m = F_m - \langle F_m\rangle$; (b) $\langle (\delta F_m)^2\rangle \sim 1$; and (c)

$$\frac{\langle [F_m(\overline{u}_1,\ldots,\overline{u}_n + \Delta\overline{u}_n,\ldots) - F_m(\overline{u}_1,\ldots,\overline{u}_n,\ldots)]^2\rangle}{\langle (\delta F_m)^2\rangle} \sim (\Delta\overline{u}_n)^2. \tag{15}$$

Equation (15) means that the characteristic period of random oscillations of F_m as a function of $\overline{u}_n$ is of order unity, $\Delta\overline{u}_n \sim 1$. In anticipation of these results we have introduced the factor $m^{1/3}$ in Eq. (12).

Consider Eq. (14) with large enough $m_1 > M = \gamma^{3/4}$. Since the factor $\gamma^{-1/2} m_1^{2/3}$ in the right-hand side of Eq. (14) is much less than unity, this equation has a unique solution at fixed $\overline{u}_k$ with $k \neq m_1$. Therefore, to estimate the number of solutions of the set of Eq. (14) in the case $\gamma \gg 1$ we have to take into account only a subset of Eq. (14) with $m < M$.

For example, at $\gamma \sim 1$ modes with $m \simeq 1$ are the most important for determination of the number of solutions of Eq. (14) and (1). This also follows, for example, from the long range $\boldsymbol{r} - \boldsymbol{r}_1$ dependence of $K^0(\boldsymbol{r},\boldsymbol{r}_1)$ and from the fact that the main contribution to Eq. (9) and the diagrams shown in Figs. 2(d)–2(g) is from integration over intermediate coordinates with $|\boldsymbol{r} - \boldsymbol{r}'| \sim L$.

Therefore we introduce a model which captures the main features of the problem at $\gamma \sim 1$: In Eq. (14) with $m = 1$ we put $\overline{u}_{m>1} = \langle \overline{u}_{m>1}\rangle = \gamma^{1/2} m^{-2/3} \langle F_m\rangle$ and get the equation with one variable $\overline{u}_1$

$$\gamma^{-1/2} \overline{u}_1 = F_1(\overline{u}_1). \tag{16}$$

It is equivalent (up to a numerical factor) to substitution in

Eq. (1) $\beta n(\boldsymbol{r}) \to (\beta/v) \int n(\boldsymbol{r})\, d\boldsymbol{r}$, where v is the sample volume. [Then expanding Eq. (1) with respect to powers of β one can reproduce the values of the diagrams Figs. 2(b)–2(g) with the precision of the factor of order of unity.] In Fig. 1 we show a qualitative "graphical" solution of Eq. (16) which corresponds to the intersection of two functions: $F_1(\overline{u}_1)$ and $\gamma^{-1/2}\overline{u}_1$. It follows from Fig. 1 (see line 3) that at $\gamma > 1$ both Eq. (16) and, consequently, Eq. (1), have many solutions. In this case the sensitivity, defined as $(\tau f/\tau_D)^2 K(\boldsymbol{r},\boldsymbol{r}')$, diverges. The main contribution to this divergency comes from realizations of $u(\boldsymbol{r})$, when $F_1(\overline{u}_1)$ and $\gamma^{-1/2}\overline{u}_1$ are tangent to each other (see line 2 in Fig. 1) and a small perturbation of, for example, the scattering potential $u(\boldsymbol{r})$ leads to a disappearance of the solution. The criterion $\gamma > 1$ is equivalent to the inequality $\langle[(\beta/L^3)(d/d\epsilon)\int n(\boldsymbol{r})\, d\boldsymbol{r}]^2\rangle > 1$. In such a form this criterion is similar to the criterion of Stoner ferromagnetic instability in metals [12].

We mention that even at $\gamma < 1$ there are rear realizations of $u(\boldsymbol{r})$ which correspond to several solutions of Eq. (1). Therefore, formally speaking, the sensitivity diverges at any γ. Obviously the conventional diagram technique is unable to describe the existence of many solutions of Eq. (1).

At $\gamma \gg 1$ the number of solutions of Eq. (16) shown in Fig. 1 is of order $\gamma^{1/2}$. However, if $\gamma \gg 1$ not only $\overline{u}_1$ but also higher modes with $1 < m < M$ are relevant. In this case Eq. (14) has multiple solutions in the intervals $|\overline{u}_m| < \gamma^{1/2} m^{-2/3}$. Since both the amplitude of fluctuations and the periods in mth direction of randomly rippled hypersurfaces $F_m(\overline{u}_1, \ldots, \overline{u}_k, \ldots)$ are of order unity, the number of solutions N of Eqs. (14) and (1) is proportional to the volume of the manifold $|\overline{u}_m| < \gamma^{1/2} m^{-2/3}$, $m < M$. As a result we have

$$N \sim \gamma^{M/2} \prod_1^M m^{-2/3} = \exp(a\gamma^{3/4}), \tag{17}$$

where $a \sim 1$. Since the problem has multiple solutions we have to redefine the concept of the sensitivity. Consider, for example, the case where the angle of the wave incidence θ is changing and suppose that a solution of Eq. (1) is following this change adiabatically. Then an exponentially small change in $\theta \sim \exp(-a\gamma^{3/4})$ will lead to the disappearance of the solution (see, for example, line 3 in Fig. 1) and the system will exhibit a jump in other solutions.

A phenomenon, similar to that considered above, may occur in disordered metals with interacting electrons. The system can be unstable with respect to the creation of random magnetic moments. In this case $n(\boldsymbol{r})$ would play the role of magnetization density. This would correspond to Finkelshtein's scenario [13]. However, in this case to get a self-consistency equation for $n(\boldsymbol{r})$ we have to integrate over electron energies up to the Fermi energy, which decreases the amplitude of mesoscopic fluctuations of $n(\boldsymbol{r})$. As a result, at small electron-electron interaction constant the situation with many solutions occurs only in the $D = 2$ case and the characteristic spatial scale of integration over $\boldsymbol{r}$ will be of the order of the localization length in the linear problem. This is the reason why the problem of interacting electrons in disordered metals remains unsolved.

Above we considered the case when $\phi(\boldsymbol{r},t) = \phi(\boldsymbol{r},\epsilon)\exp(i\epsilon t)$ is a complex quantity and $n(\boldsymbol{r}) = |\phi(\boldsymbol{r},t)|^2$ is time independent. Therefore the third harmonic, proportional to $\exp(3i\epsilon t)$, is not generated. In the case of propagation of electromagnetic waves in nonlinear media $\phi(\boldsymbol{r})$ should be considered as a real quantity, which leads to the generation of third harmonics. In this case the consideration presented above is valid only as long as the amplitude of the third harmonic is smaller than the amplitude of the first harmonic. It is the case provided that $kl^2\gamma/L \ll 1$. The latter criterion does not contradict the requirement $\gamma \gg 1$.

Finally, we mention that the problem considered above is similar to the problem of classical chaos, where the sensitivity of trajectories of motion to changes in boundary conditions exponentially increases with the sample size (see, for example, [14]).

The work of B. S. was supported by Division of Material Sciences, U.S. National Science Foundation under Contract No. DMR-9625370. The work of A. Z. was supported by Russian Fund of Fundamental Investigations under Grant No. 97-02-18078.

[1] P. A. Lee and A. D. Stone, Phys. Rev. Lett. **55**, 1622 (1985).
[2] B. Altshuler and B. Spivak, JETP Lett. **42**, 447 (1986).
[3] S. Feng, P. Lee, and A. D. Stone, Phys. Rev. Lett. **56**, 1560 (1986).
[4] B. Spivak and A. Zyuzin, in *Mesoscopic Phenomena in Solids*, edited by B. Altshuler, P. Lee, and R. Webb, Modern Problems in Condensed Matter Sciences Vol. 30 (North-Holland, Amsterdam, 1991).
[5] B. Simons and B. Altshuler, Phys. Rev. Lett. **70**, 4063 (1993).
[6] L. Landau and E. Lifshitz, *Electrodynamics of Continuous Media* (Pergamon, Oxford, 1968).
[7] V. E. Zakharov, V. S. Lvov, and G. Falkovich, *Kolmogorov Spectra of Turbulence* (Springer-Verlag, Berlin, 1992).
[8] B. B. Kadomzev, *Collective Phenomena in Plasma* (Nauka, Moscow, 1976).
[9] A. Abrikosov, L. Gorkov, and I. Dzyialoshinski, *Methods of Quantum Field Theory in Statistical Physics* (Prentice-Hall, Englewood Cliffs, N.J., 1963).
[10] In the case of $\beta > 0$ this criterion corresponds to the requirement that the self-focusing of the wave does not take place on the distance of order of l [6].
[11] A. Zyuzin and B. Spivak, Sov. Phys. JETP **66**, 560 (1987).
[12] A. A. Abrikosov, *Fundamentals of the Theory of Metals* (North-Holland, Amsterdam, 1988).
[13] A. M. Finkelshtein, Sov. Sci. Rev. A, Phys. Rev. **14**, 1 (1990).
[14] A. J. Lichtenberg and M. A. Lieberman, *Regular and Stochastic Motion* (Springer-Verlag, New York, 1992).